fractal and fractional

Article

Numerical Approximation of the Fractional Rayleigh–Stokes Problem Arising in a Generalised Maxwell Fluid

Le Dinh Long [1,2], Bahman Moradi [3], Omid Nikan [3], Zakieh Avazzadeh [4] and António M. Lopes [5,*]

1 Division of Applied Mathematics, Science and Technology Advanced Institute, Van Lang University, Ho Chi Minh City 700000, Vietnam; ledinhlong@vlu.edu.vn
2 Faculty of Applied Technology, School of Engineering and Technology, Van Lang University, Ho Chi Minh City 700000, Vietnam
3 School of Mathematics, Iran University of Science and Technology, Narmak, Tehran 16846-13114, Iran; kbccokr@gmail.com (B.M.); omidnikanmath90@gmail.com (O.N.)
4 Department of Applied Mathematics, Xi'an Jiaotong–Liverpool University, Suzhou 215123, China; zakieh.avazzadeh@xjtlu.edu.cn
5 Institute of Mechanical Engineering, Faculty of Engineering, University of Porto, 4200-465 Porto, Portugal
* Correspondence: aml@fe.up.pt

Abstract: This paper presents a numerical technique to approximate the Rayleigh–Stokes model for a generalised Maxwell fluid formulated in the Riemann–Liouville sense. The proposed method consists of two stages. First, the time discretization of the problem is accomplished by using the finite difference. Second, the space discretization is obtained by means of the predictor–corrector method. The unconditional stability result and convergence analysis are analysed theoretically. Numerical examples are provided to verify the feasibility and accuracy of the proposed method.

Keywords: fractional Rayleigh–Stokes problem; predictor–corrector method; finite difference; error estimation

Citation: Long, L.D.; Moradi, B.; Nikan, O.; Avazzadeh, Z.; Lopes, A.M. Numerical Approximation of the Fractional Rayleigh–Stokes Problem Arising in a Generalised Maxwell Fluid . *Fractal Fract.* **2022**, *6*, 377. https://doi.org/10.3390/fractalfract6070377

Academic Editor: Haci Mehmet Baskonus

Received: 10 June 2022
Accepted: 30 June 2022
Published: 2 July 2022

1. Introduction

Fractional calculus (FC) generalises the classical integer-order calculus [1,2]. In the last decade, FC has received considerable attention in a variety of scientific areas [3–6]. In most cases, it is difficult to compute an explicit solution to fractional differential equations, which has attracted researchers to look for accurate and efficient numerical approaches for solving these Equations [7–14].

FC has successfully described viscoelastic fluid constitutive relations [15–17]. One usually starts the process of modelling viscoelastic fluids via fractional derivatives by modifying a traditional differential equation. This generalisation involves using the Riemann–Liouville (R–L) fractional derivative operator instead of the standard time derivative. Shen et al. [18] derived the Rayleigh–Stokes Equation (RSE) for a generalised fluid of the second grade flowing within a heated edge and over a heated flat plate. The analytic solutions for the temperature and velocity fields were obtained via the fractional Laplace and the Fourier sine transforms. Mainardi [19] provided a comprehensive review of the relationship between FC and viscoelastic models, linear viscoelasticity, and wave propagation. Qi and Xu [20] studied an unsteady flow of fractional Maxwell fluid in a channel. Xue and Nie [21] addressed the RSE to a heated generalised fluid of the second grade with fractional derivative flows inside a porous half-space.

In this paper, we investigate the numerical solution for the time fractional Rayleigh–Stokes Equation (TFRSE) including the time fractional derivative

$$\begin{aligned}\frac{\partial v(x,y,t)}{\partial t} &= {}_0D_t^{1-\gamma}\left[k_1\frac{\partial^2 v(x,y,t)}{\partial x^2} + k_2\frac{\partial^2 v(x,y,t)}{\partial y^2}\right] \\ &\quad + k_3\frac{\partial^2 v(x,y,t)}{\partial x^2} + k_4\frac{\partial^2 v(x,y,t)}{\partial y^2} + f(x,y,t),\end{aligned} \tag{1}$$

with initial and boundary conditions (abbreviated as IC and BCs, respectively):

$$v(x,y,0) = \phi(x,y), \quad 0 \le x,y \le L, \tag{2}$$
$$v(x,0,t) = \varphi_1(x,t), \quad v(x,L,t) = \varphi_2(x,t), \quad 0 \le t \le T, \quad 0 \le x \le L, \tag{3}$$
$$v(0,y,t) = \psi_1(y,t), \quad v(L,y,t) = \psi_2(y,t), \quad 0 \le t \le T, \quad 0 \le y \le L, \tag{4}$$

where $v(x,y,t)$ represent the velocity field, the coefficients k_1, k_2, k_3 and k_4 are positive constants, $0 < \gamma < 1$, $f(x,y,t)$ is a source term, functions ϕ, φ_1, φ_2, ψ_1 and ψ_2 are prescribed and ${}_0D_t^{1-\gamma}v(x,y,t)$ is the R–L fractional differential derivative of order $1-\gamma$ denoted by

$${}_0D_t^{1-\gamma}v(x,y,t) = \frac{1}{\Gamma(\gamma)}\frac{\partial}{\partial t}\int_0^t \frac{v(x,y,\eta)}{(t-\eta)^{1-\gamma}}\mathrm{d}\eta. \tag{5}$$

Some numerical techniques have been used to approximate the TFRSE Equation (1). Chen et al. [22] formulated an implicit finite difference (FD) algorithm. Wu [23] presented an implicit numerical approximation scheme. Jiang and Lin [24] proposed a numerical technique based on the method of reproducing kernel. Mohebbi et al. [25] adopted the compact FD method (CFDM) and radial basis function (RBF) meshless method (RMM). Zaky [26] and Shivanian et al. [27] used the Legendre–Tau and the meshless singular boundary methods, respectively. Hafez et al. [28] applied the Jacobi Spectral Galerkin method for the distributed TFRSE. Safari and HongGuang [29] adopted the improved dual reciprocity and singular boundary schemes for the TFRSE, while Golbabai et al. [30] proposed the local meshless RBF. Khan et al. [31] developed the high-order compact scheme, whereas Naz et al. [32] advanced a modified implicit scheme for the TFRSE.

This paper introduces a numerical method for the TFRSE and is organized as follows. Section 2 describes an algorithm to approximate the time fractional derivative of the TFRSE Equation (1). Section 3 accomplishes the space discretization with the help of the predictor–corrector method. Section 4 studies the unconditional stability result and convergence analysis of the proposed strategy by using Fourier analysis. Section 5 reports the numerical examples of the TFRSE and verifies the efficiency of the proposed scheme. Finally, Section 6 provides a concise conclusion.

2. The Time Discretization

Let us define $t_k = k\tau$, where $\tau = \frac{T}{N}$ represents the time step size for $k = 0,1,2,\ldots,N$. We suppose that the solution $u(x,y,t)$ has a continuous partial derivative $\frac{\partial u(x,y,t)}{\partial t}$ for $t \ge 0$, and that the R–L fractional derivative ${}_0D_t^{1-\gamma}u(x,y,t)$ can be evaluated using the Grünwald–Letnikov (G–L) formulation [33], described as

$${}_0D_t^{1-\gamma}u(x,y,t) = \frac{1}{\tau^{1-\gamma}}\sum_{j=0}^{[t/\tau]}\lambda_j^{(1-\gamma)}u(x,y,t-j\tau) + \mathcal{O}(\tau^q), \qquad 0<\gamma<1, \quad 0<q<1, \tag{6}$$

so that $\lambda_j^{(1-\gamma)}$ correspond to the coefficients of the generating function

$$\lambda(z,1-\gamma) = \sum_{j=0}^{\infty}\lambda_j^{(1-\gamma)}z^j,$$

where the coefficients $\lambda_0^{(1-\gamma)} = 1$ and $\lambda_j^{(1-\gamma)} = (-1)^j \binom{1-\gamma}{j}$ are the normalized G–L weights. The coefficients can be obtained recursively as:

$$\lambda_0^{(1-\gamma)} = 1, \quad \lambda_j^{(1-\gamma)} = \left(1 - \frac{2-\gamma}{j}\right)\lambda_{j-1}^{(1-\gamma)}, \qquad j \geq 1.$$

The $\lambda_j^{1-\gamma}$ have some useful properties, as given by Lemma 1 ([33]).

Lemma 1. The coefficients $\lambda_j^{1-\gamma}$ introduced in Equation (6) satisfy

1. $\lambda_j^{(1-\gamma)} < 0, \qquad j = 1, 2, \dots .$
2. $\sum_{j=0}^{\infty} \lambda_j^{(1-\gamma)} = 0, \qquad \forall n \in \mathbb{N}, \quad -\sum_{j=0}^{n} \lambda_j^{(1-\gamma)} < 1$ and $\sum_{j=0}^{n-1} \lambda_j^{(1-\gamma)} > 0.$
3. $\sum_{j=n}^{\infty} \lambda_j^{(1-\gamma)} \geq \frac{1}{n^{1-\gamma}\Gamma(\gamma)}.$

Let us consider the following notations:

$$\left[{}_0D_t^{1-\gamma} v(x,y,t)\right]_{t=t_k} = \tau^{\gamma-1} \sum_{l=0}^{k} \lambda_l v(x,y,t_{k-l}) + \mathcal{O}(\tau), \tag{7}$$

$$\frac{\partial v(x,y,t_k)}{\partial t} = \frac{v(x,y,t_k) - v(x,y,t_{k-1})}{\tau} + \mathcal{O}(\tau). \tag{8}$$

Now, we can formulate the semi-time discretization scheme for Equation (1) by means of the aforementioned relations

$$\begin{aligned} \frac{v(x,y,t_k) - v(x,y,t_{k-1})}{\tau} &= \tau^{\gamma-1} \sum_{l=0}^{k} \lambda_l \left(k_1 \frac{\partial^2 v(x,y,t_{k-l})}{\partial x^2} + k_2 \frac{\partial^2 v(x,y,t_{k-l})}{\partial y^2} \right) \\ &+ \left(k_3 \frac{\partial^2 v(x,y,t_{k-l})}{\partial x^2} + k_4 \frac{\partial^2 v(x,y,t_{k-l})}{\partial y^2} \right) + f(x,y,t_k). \end{aligned} \tag{9}$$

3. The Space Discretization

Let $\Omega = \{(x_i, y_j) |\, 1 \leq i \leq M_1,\ 1 \leq j \leq M_2\}$ with $x_i = ih_x,\ y_j = jh_y$, so that $h_x = \frac{L}{M_1}$, $h_y = \frac{L}{M_2}$ represent the space steps in the x and y directions, respectively, and also M_1 and M_2 denote the total number of space steps in the x and y directions, respectively. Discretizing Equation (1) at the above grid points (x_i, x_j, t_k) and by using

$$\frac{\partial^2 v(x_i,y_j,t_k)}{\partial x^2} = \frac{\delta_x^2 v(x_i,y_j,t_k)}{h_x^2} + \mathcal{O}(h_x^2), \tag{10}$$

$$\frac{\partial^2 v(x_i,y_j,t_k)}{\partial y^2} = \frac{\delta_y^2 v(x_i,y_j,t_k)}{h_y^2} + \mathcal{O}(h_y^2), \tag{11}$$

where

$$\delta_x^2 v(x_i,y_j,t_k) = v(x_{i-1},y_j,t_k) - 2v(x_i,y_j,t_k) + v(x_{i+1},y_j,t_k),$$

$$\delta_y^2 v(x_i,y_j,t_k) = v(x_i,y_{j-1},t_k) - 2v(x_i,y_j,t_k) + v(x_i,y_{j+1},t_k),$$

we obtain the following corrector formula as

$$v_{i,j}^{k} = \frac{1}{\tau}\Bigg[v_{i,j}^{k-1} + \mu_1 \sum_{l=1}^{k} \lambda_l \delta_x^2 v_{i,j}^{k-l} + \mu_2 \sum_{l=1}^{k} \lambda_l \delta_y^2 v_{i,j}^{k-l} + (\mu_1+\mu_3)(v_{i+1,j}^{k} + v_{i-1,j}^{k})$$
$$+(\mu_2+\mu_4)(v_{i,j+1}^{k} + v_{i,j-1}^{k}) + \tau f_{i,j}^{k}\Bigg], \tag{12}$$
$$1 \le i \le K_1 - 1, \quad 1 \le j \le K_2 - 1, \quad 1 \le k \le N.$$

such that

$$\tau = 1 + 2(\mu_1+\mu_2+\mu_3+\mu_4),$$
$$\mu_1 = k_1 \frac{\tau^{\gamma}}{h_x^2}, \quad \mu_2 = k_2 \frac{\tau^{\gamma}}{h_y^2}, \quad \mu_3 = k_3 \frac{\tau}{h_x^2}, \quad \mu_4 = k_4 \frac{\tau}{h_y^2}, \tag{13}$$

with $f_{i,j}^{k}$ representing the value of function f at (x_i, y_j, t_k). The truncation error [22] is obtained as

$$R = \mathcal{O}(h_x^2 + h_y^2)\tau^{\gamma} \sum_{l=0}^{k} \lambda_l + \mathcal{O}(\tau h_x^2 + \tau h_y^2 + \tau^2), \tag{14}$$

and the predictor formula is denoted by

$$v_{i,j}^{k} = v_{i,j}^{k-1} - \epsilon v_{i,j}^{k-1}, \tag{15}$$
$$1 \le i \le K_1 - 1, \quad 1 \le j \le K_2 - 1, \quad 1 \le k \le N,$$

with the IC and BCs

$$v_{i,j}^{0} = \phi(x_i, y_j), \quad i = 0, 1, \ldots, K_1, \quad j = 0, 1, \ldots, K_2, \tag{16}$$
$$v_{i,0}^{k} = \varphi_1(x_i, t_k), \quad v_{i,K_2}^{k} = \varphi_2(x_i, t_k), \quad i = 1, 2, \ldots, K_1 - 1, \quad k = 1, 2, \ldots, N, \tag{17}$$
$$v_{0,j}^{k} = \psi_1(y_j, t_k), \quad v_{K_1,j}^{k} = \psi_2(y_j, t_k), \quad j = 1, 2, \ldots, K_2 - 1, \quad k = 1, 2, \ldots, N, \tag{18}$$

respectively. We can adopt the following iterative procedure to approximate Equation (1) with Equations (2)–(4).

P: Predict some value $[v_{i,j}^{k}]^0$ for $v_{i,j}^{k}$ with

$$[v_{i,j}^{k}]^0 = v_{i,j}^{k-1} - \epsilon v_{i,j}^{k-1}$$
$$1 \le i \le K_1 - 1, \quad 1 \le j \le K_2 - 1, \quad 1 \le k \le N,$$

where ϵ is a very small number.

E: Evaluate the implicit part in Equation (12) with $[v_{i,j}^{k}]^0$.

C: Correct $[v_{i,j}^{k}]^0$ to obtain a new $[v_{i,j}^{k}]^1$ for $v_{i,j}^{k}$ with

$$[v_{i,j}^{k}]^1 = \frac{1}{\tau}\Bigg[v_{i,j}^{k-1} + \mu_1 \sum_{l=1}^{k} \lambda_l \delta_x^2 v_{i,j}^{k-l} + \mu_2 \sum_{l=1}^{k} \lambda_l \delta_y^2 v_{i,j}^{k-l} + (\mu_1+\mu_3)([v_{i+1,j}^{k}]^0 + [v_{i-1,j}^{k}]^0)$$
$$+(\mu_2+\mu_4)([v_{i,j+1}^{k}]^0 + [v_{i,j-1}^{k}]^0) + \tau f_{i,j}^{k}\Bigg],$$
$$1 \le i \le K_1 - 1, \quad 1 \le j \le K_2 - 1, \quad 1 \le k \le N.$$

E: Evaluate the implicit part in Equation (12) with $[v_{i,j}^{k}]^1$.

C: Correct $[v_{i,j}^{k}]^1$ with

$$[v_{i,j}^k]^2 = \frac{1}{\tau}\Bigg[v_{i,j}^{k-1} + \mu_1 \sum_{l=1}^{k} \lambda_l \delta_x^2 v_{i,j}^{k-l} + \mu_2 \sum_{l=1}^{k} \lambda_l \delta_y^2 v_{i,j}^{k-l} + (\mu_1+\mu_3)([v_{i+1,j}^k]^1 + [v_{i-1,j}^k]^1)$$
$$+(\mu_2+\mu_4)([v_{i,j+1}^k]^1 + [v_{i,j-1}^k]^1) + \tau f_{i,j}^k\Bigg],$$
$$1 \le i \le K_1 - 1, \quad 1 \le j \le K_2 - 1, \quad 1 \le k \le N.$$

$\vdots$

The sequence of operations

$$\text{PECECECEC}\ldots$$

determines $v_{i,j}^k$ for a sequence of values as

$$[v_{i,j}^k]^0, [v_{i,j}^k]^1, [v_{i,j}^k]^2, \ldots$$

An appropriate stop condition is

$$\left|[v_{i,j}^k]^{n+1} - [v_{i,j}^k]^n\right| < \varepsilon, \qquad n = 0,1,2,\ldots$$

where n is the number of iterations. Hence, the relation Equation (12) can be rewritten in following form:

$$\begin{cases} [v_{i,j}^k]^P = v_{i,j}^{k-1} - \epsilon v_{i,j}^{k-1} \\ [v_{i,j}^k]^C = \frac{1}{\tau}\Bigg[v_{i,j}^{k-1} + \mu_1 \sum_{l=1}^{k} \lambda_l \delta_x^2 v_{i,j}^{k-l} + \mu_2 \sum_{l=1}^{k} \lambda_l \delta_y^2 v_{i,j}^{k-l} + (\mu_1+\mu_3)([v_{i+1,j}^k]^P + [v_{i-1,j}^k]^P) \\ \qquad + (\mu_2+\mu_4)([v_{i,j+1}^k]^P - [v_{i,j-1}^k]^P) + \tau f_{i,j}^k\Bigg], \end{cases} \tag{19}$$
$$1 \le i \le K_1 - 1, \quad 1 \le j \le K_2 - 1, \quad 1 \le k \le N,$$

with the IC and BCs Equations (16)–(18).

4. Theoretical Analysis of the Proposed Method

4.1. Stability Analysis

We now examine the stability of the proposed method Equation (19) by using Fourier analysis. Let $v_{i,j}^k$ and $\bar{v}_{i,j}^k$ be the exact and the approximated solutions for $[v_{i,j}^k]^C$ in Equation (19). Then, the error can be defined as:

$$E_{i,j}^k = v_{i,j}^k - \bar{v}_{i,j}^k.$$

We can obtain for corrector formula

$$E_{i,j}^k = \frac{1}{\tau}\Bigg[E_{i,j}^{k-1} + \mu_1 \sum_{l=1}^{k} \lambda_l \delta_x^2 E_{i,j}^{k-l} + \mu_2 \sum_{l=1}^{k} \lambda_l \delta_y^2 E_{i,j}^{k-l} + (\mu_1+\mu_3)(E_{i+1,j}^k + E_{i-1,j}^k)$$
$$+ (\mu_2+\mu_4)(E_{i,j+1}^k + E_{i,j-1}^k)\Bigg]. \tag{20}$$

Let us introduce the following function:

$$E^k(x,y) = \begin{cases} E_{i,j}^k & (x,y) \in \Omega_1, \\ 0 & (x,y) \in \Omega_2, \end{cases}$$

such that

$$\Omega_1 = \left\{ (x,y) \middle| x_{i-\frac{1}{2}} < x \leq x_{i+\frac{1}{2}}, \quad y_{j-\frac{1}{2}} < y \leq y_{j+\frac{1}{2}} \right\},$$

$$\Omega_2 = \left\{ (x,y) \middle| 0 \leq x \leq \frac{h_x}{2} \quad \text{or } L - \frac{h_x}{2} < x \leq L \quad \text{or } 0 \leq y \leq \frac{h_y}{2} \quad \text{or } L - \frac{h_y}{2} < y \leq L \right\}.$$

Then, $E^k(x,y)$ can be approximated by using the Fourier series as

$$E^k(x,y) = \sum_{l_1=-\infty}^{+\infty} \sum_{l_2=-\infty}^{+\infty} \zeta_k(l_1,l_2) e^{2\pi I \frac{(l_1 x + l_2 y)}{L}} \quad 1 \leq k \leq N,$$

where

$$\zeta_k(l_1,l_2) = \frac{1}{L^2} \int_0^L \int_0^L E^k(x,y) e^{-2\pi I \frac{l_1 x + l_2 y}{L}} \mathrm{d}x\mathrm{d}y, \quad I = \sqrt{-1}.$$

Applying Parseval equality for $k = 0, 1, \ldots, N$

$$||E^k||_2 = \left[\sum_{i=1}^{K_1-1} \sum_{j=1}^{K_2-1} h_x h_y |E^k_{i,j}|^2 \right]^{\frac{1}{2}} = \left[\sum_{l_1=-\infty}^{\infty} \sum_{l_2=-\infty}^{\infty} |\zeta_k(l_1,l_2)|^2 \right]^{\frac{1}{2}}. \tag{21}$$

Suppose that the difference Equation (20) has the following solution

$$E^k_{i,j} = \zeta_k e^{I(\sigma_1 i h_x + \sigma_2 j h_y)}, \tag{22}$$

where $\sigma_1 = \frac{2\pi l_1}{L}$ and $\sigma_2 = \frac{2\pi l_2}{L}$. Substituting Equation (22) into Equation (20) and simplifying leads to

$$\zeta_k = \frac{1}{\tau} \left[\zeta_{k-1} - \psi \sum_{l=1}^{k} \lambda_l \zeta_{k-l} + \phi \zeta_k \right], \tag{23}$$

such that

$$\psi = 4\mu_1 \sin^2 \frac{\sigma_1 h_x}{2} + 4\mu_2 \sin^2 \frac{\sigma_2 h_y}{2},$$
$$\phi = 2(\mu_1 + \mu_3)(1 - 2\sin^2 \frac{\sigma_1 h_x}{2}) + 2(\mu_2 + \mu_4)(1 - 2\sin^2 \frac{\sigma_2 h_y}{2}).$$

Now, we investigate the stability of the method Equation (19).

Theorem 1. The predictor–corrector method Equation (19) is stable if and only if $\phi \geq 0$.

Proof. The proof will be obtained by using mathematical induction. For $k = 1$, we get

$$|\zeta_1| = \frac{1}{\tau} |[1 - \psi(\gamma - 1) + \phi]| |\zeta_0| \leq \frac{1}{\tau} [1 - \psi|(\gamma - 1)| + \phi] |\zeta_0| \leq |\zeta_0|. \tag{24}$$

Assume that

$$|\zeta_k| \leq |\zeta_0|, \qquad k = 1, 2, \ldots, N-1. \tag{25}$$

Then, by using [Lemma 2 in [25]], we arrive at

$$\begin{aligned}
|\zeta_k| &= \left|\frac{1}{\tau}\left[\zeta_{k-1} - \psi\sum_{l=1}^{k}\lambda_l\zeta_{k-l} + \phi\zeta_k\right]\right|, \\
&\leq \frac{1}{\tau}\left[1 - \psi\left|\sum_{l=1}^{k}\lambda_l\right| + \phi\right]|\zeta_0|, \\
&= \frac{1}{\tau}\left[1 + \psi\sum_{l=1}^{k}\lambda_l + \phi\right]|\zeta_0|, \\
&\leq \frac{1}{\tau}(1 - \psi + \phi)|\zeta_0|, \\
&\leq |\zeta_0|.
\end{aligned}$$

Using the Parseval equality Equation (21), the error in the solution of the difference Equation (23) satisfies

$$||E^k||_2 \leq ||E^0||_2 \quad , k = 1, 2, \ldots, N.$$

The proof of the theorem is completed. □

4.2. Convergence Analysis

Let us define the truncation error in the proposed method to satisfy the following form

$$\begin{aligned}
R_{i,j}^k =& v(x_i, y_j, t_k) - v(x_i, y_j, t_{k-1}) - \mu_1\sum_{l=0}^{k}\lambda_l\delta_x^2 v(x_i, y_j, t_{k-l}) - \mu_2\sum_{l=0}^{k}\lambda_l\delta_y^2 v(x_i, y_j, t_{k-l}) \\
&-\mu_3\delta_x^2 v(x_i, y_j, t_k) - \mu_4\delta_x^2 v(x_i, y_j, t_k) - \tau f(x_i, y_j, t_k),
\end{aligned} \tag{26}$$

$$1 \leq i \leq K_1 - 1, \quad 1 \leq j \leq K_2 - 1, \quad 1 \leq k \leq N.$$

From Lemma 3 in [25], we have

$$R_{i,j}^k = \mathcal{O}(\tau h_x^2 + \tau h_y^2 + \tau^2),$$

or

$$|R_{i,j}^k| \leq C_1(\tau h_x^2 + \tau h_y^2 + \tau^2). \tag{27}$$

$$1 \leq i \leq K_1 - 1, \quad 1 \leq j \leq K_2 - 1, \quad 1 \leq k \leq N,$$

where $C_1 \in \mathbb{R}^+$. Subtracting Equation (12) from Equation (26), we get

$$\begin{aligned}
e_{i,j}^k =& \frac{1}{\tau}\Bigg[e_{i,j}^{k-1} + \mu_1\sum_{l=1}^{k}\lambda_l\delta_x^2 e_{i,j}^{k-l} + \mu_2\sum_{l=1}^{k}\lambda_l\delta_y^2 e_{i,j}^{k-l} + (\mu_1 + \mu_3)(e_{i+1,j}^k + e_{i-1,j}^k) \\
&+ (\mu_2 + \mu_4)(e_{i,j+1}^k + e_{i,j-1}^k) + R_{i,j}^k\Bigg],
\end{aligned} \tag{28}$$

where $e_{i,j}^k = v(x_i, y_j, t_k) - v_{i,j}^k$, and

$$e_{0,j}^k = e_{K_1,j}^k = 0, \quad e_{i,0}^k = e_{i,K_2}^k = 0, \quad e_{i,j}^0 = 0,$$

$$1 \leq i \leq K_1, \quad 1 \leq j \leq K_2, \quad 1 \leq k \leq N.$$

Let us consider the following two functions:

$$e^k(x, y) = \begin{cases} e_{i,j}^k, & (x, y) \in \Omega_1, \\ 0, & (x, y) \in \Omega_2, \end{cases}$$

and

$$R^k(x,y) = \begin{cases} R^k_{i,j}, & (x,y) \in \Omega_1, \\ 0, & (x,y) \in \Omega_2. \end{cases}$$

Then, $e^k_{i,j}$ and $R^k_{i,j}$ can by approximated by the Fourier series

$$e^k(x,y) = \sum_{l_1=-\infty}^{+\infty} \sum_{l_2=-\infty}^{+\infty} \alpha_k(l_1,l_2) e^{2\pi I \frac{(l_1 x + l_2 y)}{L}} \qquad 0 \le k \le N,$$

$$R^k(x,y) = \sum_{l_1=-\infty}^{+\infty} \sum_{l_2=-\infty}^{+\infty} \beta_k(l_1,l_2) e^{2\pi I \frac{(l_1 x + l_2 y)}{L}} \qquad 0 \le k \le N,$$

in which

$$\alpha_k(l_1,l_2) = \frac{1}{L^2} \int_0^L \int_0^L e^k(x,y) e^{-2\pi I \frac{l_1 x + l_2 y}{L}} \mathrm{d}x\mathrm{d}y$$

and

$$\beta_k(l_1,l_2) = \frac{1}{L^2} \int_0^L \int_0^L R^k(x,y) e^{-2\pi I \frac{l_1 x + l_2 y}{L}} \mathrm{d}x\mathrm{d}y.$$

Moreover, we can obtain the values of $||e^k||_2$ and $||R^k||_2$ for $k = 0, 1, \ldots, N$ as

$$||e^k||_2 = \left[\sum_{i=1}^{K_1-1} \sum_{j=1}^{K_2-1} h_x h_y |e^k_{i,j}|^2 \right]^{\frac{1}{2}} = \left[\sum_{l_1=-\infty}^{\infty} \sum_{l_2=-\infty}^{\infty} |\alpha_k(l_1,l_2)|^2 \right]^{\frac{1}{2}}, \tag{29}$$

and

$$||R^k||_2 = \left[\sum_{i=1}^{K_1-1} \sum_{j=1}^{K_2-1} h_x h_y |R^k_{i,j}|^2 \right]^{\frac{1}{2}} = \left[\sum_{l_1=-\infty}^{\infty} \sum_{l_2=-\infty}^{\infty} |\beta_k(l_1,l_2)|^2 \right]^{\frac{1}{2}}. \tag{30}$$

Suppose that $e^k_{i,j}$ and $R^k_{i,j}$ have the following form

$$e^k_{i,j} = \alpha_k e^{I(\sigma_1 i h_x + \sigma_2 j h_y)}, \quad R^k_{i,j} = \beta_k e^{I(\sigma_1 i h_x + \sigma_2 j h_y)}, \tag{31}$$

where

$$\sigma_1 = \frac{2\pi l_1}{L}, \quad \sigma_2 = \frac{2\pi l_2}{L}.$$

Substituting Equation (31) into Equation (28) gives

$$\alpha_k = \frac{1}{\tau} \left[\alpha_{k-1} - \psi \sum_{l=1}^{k} \lambda_l \alpha_{k-l} + \phi \alpha_k + \beta_k \right], \tag{32}$$

where τ, ψ and ϕ are as defined before. By virtue of the relations Equations (27) and (30), we get

$$\begin{aligned} ||R^k||_2 &\le \sqrt{K_1 h_x} \sqrt{K_2 h_y} C_1 (\tau h_x^2 + \tau h_y^2 + \tau^2), \\ &= C_1 L (\tau h_x^2 + \tau h_y^2 + \tau^2). \end{aligned} \tag{33}$$

Based on [22], it holds that

$$|\beta_k| \equiv |\beta_k(l_1,l_2)| \le C_2 |\beta_1| \equiv C_2 |\beta_1(l_1,l_2)| \quad k = 1, 2, \ldots, N, \tag{34}$$

where $C_2 \in \mathbb{R}^+$.

Proposition 1. Let α_k denote the solutions of Equation (32). Then, we have

$$|\alpha_k| \leq C_2 k|\beta_1|, \quad 1 \leq k \leq N,$$

where $C_2 \in \mathbb{R}^+$.

Proof. The principle of mathematical induction is applied by considering $e^0 = 0$, which leads to

$$\alpha_0 \equiv \alpha_0(l_1, l_2) = 0.$$

For $k = 1$, we obtain

$$|\alpha_1| \leq |\frac{1}{\tau}||\beta_1| \leq |\beta_1| \leq C_2|\beta_1|.$$

Let us assume that

$$|\alpha_n| \leq nC_2|\beta_1| \quad 1 \leq n \leq k-1.$$

Then, based on Lemma in [25], we can conclude that

$$\begin{aligned} |\alpha_k| &\leq \frac{1}{\tau}\left[(k-1) - \psi(k-1)\sum_{l=1}^{k}|\lambda_l| + \phi(k-1) + 1\right]C_2|\beta_1|, \\ &\leq \frac{1}{\tau}\left[k - \psi(k-1) + \phi(k-1)\right]C_2|\beta_1|, \\ &\leq kC_2|\beta_1|, \end{aligned}$$

which completes the proof. □

Theorem 2. The predictor–corrector method Equation (19) is convergent with the order $\mathcal{O}(h_x^2 + h_y^2 + \tau)$.

Proof. By considering Proposition 1 and using relations Equations (32) and (33), we can obtain

$$||e^k||_2 \leq kC_2||R^1||_2 \leq kC_1C_2L(\tau h_x^2 + \tau h_y^2 + \tau),$$

and noticing that $k\tau \leq T$, then

$$||e^k||_2 \leq C(h_x^2 + h_y^2 + \tau),$$

in which

$$C = C_1C_2TL,$$

and this completes the proof. □

5. Results and Discussion

This section presents two numerical examples for illustrating the stability and accuracy of the proposed method with several values of h_x, h_y, τ and γ. For this aim, we compute the following maximum-norm error L_∞:

$$L_\infty = \max_{1 \leq j \leq N-1} |v(\mathbf{x}_j, T) - V(\mathbf{x}_j, T)|,$$

where v and V are the approximate and exact solutions, respectively. In addition, we evaluate the computational order in the time direction for the proposed method as:

$$C_\tau = \frac{\log(\frac{E_1}{E_2})}{\log(\frac{\tau_1}{\tau_2})},$$

where E_1 and E_2 represent the errors corresponding to time step with sizes τ_1 and τ_2, respectively.

Example 1. Let us consider the following TFRSE:

$$\frac{\partial v(x,y,t)}{\partial t} = {}_0D_t^{1-\gamma}\left(\frac{\partial^2 v(x,y,t)}{\partial x^2} + \frac{\partial^2 v(x,y,t)}{\partial y^2}\right) + \frac{\partial^2 v(x,y,t)}{\partial x^2} + \frac{\partial^2 v(x,y,t)}{\partial y^2} + f(x,y,t), \qquad (x,y) \in \Omega = [0,1]^2.$$

The IC and BCs as well as $f(x,y,t)$ are determined from an exact solution $v(x,y,t) = \exp(x+y)t^{1+\gamma}$.

The proposed method is implemented for solving this problem when the total time $T = 1$ with various values of h_x, h_y, τ and γ. Table 1 presents the maximum absolute errors L_∞, time convergence orders C_τ and execution times (in seconds) for $h_x = h_y = \frac{1}{8}$, $\gamma \in \{0.55, 0.85\}$ and various values of τ. We see that the obtained computational orders C_τ in time direction are close to the theoretical convergence rate, that is, $\mathcal{O}(\tau)$. Table 2 lists the maximum absolute errors L_∞ in the solution for $\gamma \in \{0.5, 0.75\}$, and several values of $h_x = h_y$ and τ. Table 3 compares the maximum absolute errors L_∞ in the solution with those resulting from the method described in [25] for $h_x = h_y = \frac{1}{16}$, $\gamma = 0.15$ and various values of τ. Table 4 makes the comparison of L_∞ errors in the solution with those resulting from the method in [25] for different values of $h_x = h_y$, $\gamma = 0.2$, and τ. Table 5 compares the maximum absolute errors L_∞ in the solution and execution times (in seconds) with those obtained with other schemes [22,25] for $h_x = h_y = \frac{1}{4}$, $\tau = \frac{1}{900}$ and different values of γ. Figure 1 shows the approximate solution and the associated computational error L_∞ of the proposed method with $\gamma = 0.85$, $K_1 = K_2 = 16$, and $N = 256$.

Table 1. The maximum absolute errors L_∞, time convergence orders C_τ and execution times (in seconds) of Example 1 for $h_x = h_y = \frac{1}{8}$ and $\gamma \in \{0.55, 0.85\}$ and different values of τ.

τ	$\gamma = 0.55$				$\gamma = 0.85$			
	n	L_∞	C_τ	CPU Time (s)	n	L_∞	C_τ	CPU Time (s)
1/8	65	6.3090×10^{-3}	–	0.1285	47	9.3000×10^{-3}	–	0.1689
1/10	63	5.3982×10^{-3}	0.69871	0.1493	47	8.9975×10^{-3}	0.14819	0.1093
1/16	65	3.7302×10^{-3}	0.78639	0.1558	48	4.8582×10^{-3}	1.31122	1.7073
1/40	66	1.6951×10^{-3}	0.86077	0.5390	44	2.3980×10^{-3}	0.77053	0.6569
1/64	64	1.1170×10^{-3}	0.88743	6.5077	40	1.5138×10^{-3}	0.97874	1.3609
1/128	70	5.6189×10^{-4}	0.99127	11.508	32	7.6491×10^{-4}	0.98481	2.1372

Table 2. The maximum absolute errors L_∞ in the solution of Example 1 for $\gamma \in \{0.5, 0.75\}$, and different values of $h_x = h_y$ and τ.

h_x	τ	$\gamma = 0.5$		$\gamma = 0.75$	
		n	L_∞	n	L_∞
1/4	1/4	8	7.9397×10^{-3}	7	1.6266×10^{-2}
1/10	1/64	117	1.2258×10^{-3}	80	1.5186×10^{-3}
1/16	1/128	419	6.7026×10^{-5}	200	7.8371×10^{-4}
1/8	1/210	387	9.6004×10^{-4}	40	8.2789×10^{-4}

Table 3. The maximum absolute errors L_∞ of Example 1 for $h_x = h_y = \frac{1}{16}$, $\gamma = 0.15$ and different values of τ.

τ	Proposed Method		RMM [25]	CFDM [25]
	n	L_∞	L_∞	L_∞
1/10	672	4.7049×10^{-3}	6.8422×10^{-3}	4.3318×10^{-3}
1/20	775	2.4089×10^{-3}	4.9548×10^{-3}	2.2982×10^{-3}
1/30	791	1.6230×10^{-3}	3.3632×10^{-3}	1.5709×10^{-3}

Table 4. The maximum absolute errors L_∞ and execution times (in seconds) of Example 1 for $\gamma = 0.2$, and different values of $h_x = h_y$ and τ.

h_x	τ	Proposed Method			CFDM [25]	
		n	L_∞	CPU Time (s)	L_∞	CPU Time (s)
1/4	1/50	13	8.8037×10^{-4}	0.8212	9.6999×10^{-4}	0.0470
1/8	1/128	116	2.0750×10^{-4}	0.9606	3.8649×10^{-4}	0.5000
1/18	1/28	900	1.7396×10^{-3}	6.3644	1.7554×10^{-3}	0.0460

Table 5. The maximum absolute errors L_∞ of Example 1 for $h_x = h_y = \frac{1}{4}$ and $\tau = \frac{1}{900}$ and different values of γ.

γ	Proposed Method		RMM [25]	CFDM [25]
	n	L_∞	L_∞	L_∞
0.7	5	8.3469×10^{-4}	5.8055×10^{-4}	1.8231×10^{-3}
0.8	4	7.0423×10^{-4}	7.3493×10^{-4}	1.8250×10^{-3}
0.9	4	9.8265×10^{-4}	9.0422×10^{-4}	1.8265×10^{-3}

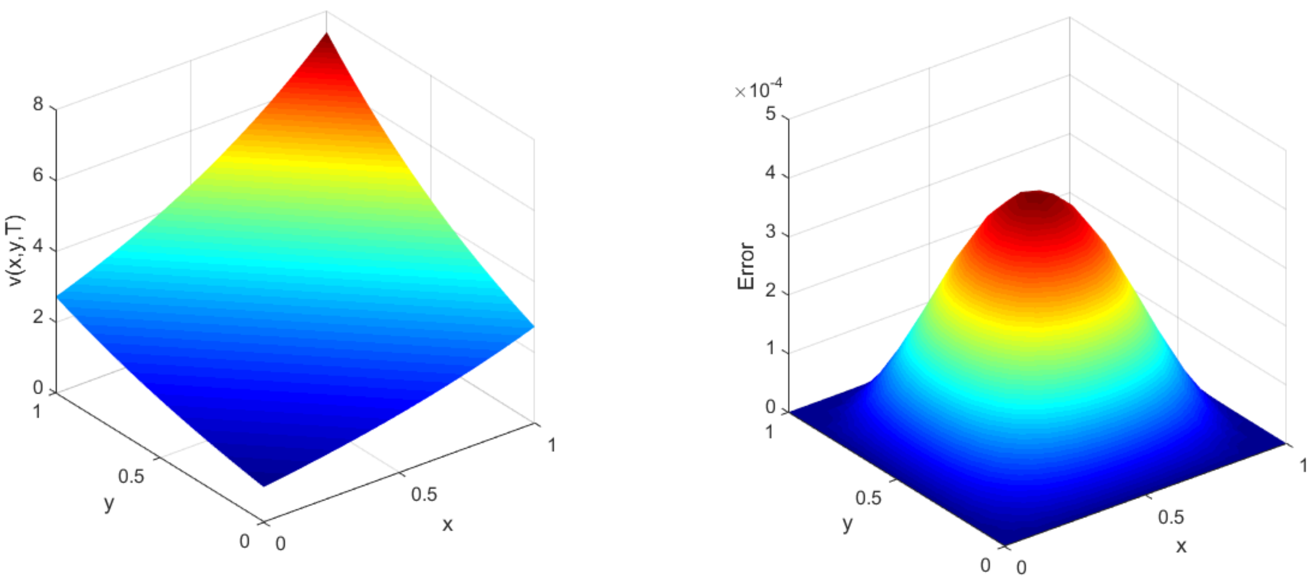

Figure 1. Approximate solution $v(x, y, T)$ and the associated computational error L_∞ of the proposed method with $\gamma = 0.85$ and $K_1 = K_2 = 16$ and $N = 256, n = 263$ (left and right panels, respectively).

Example 2. Consider the following TFRSE:

$$\frac{\partial v(x,y,t)}{\partial t} = {}_0D_t^{1-\gamma}\left(\frac{\partial^2 v(x,y,t)}{\partial x^2} + \frac{\partial^2 v(x,y,t)}{\partial y^2}\right) + \frac{\partial^2 v(x,y,t)}{\partial x^2} + \frac{\partial^2 v(x,y,t)}{\partial y^2} + f(x,y,t), \qquad (x,y) \in \Omega = [0,1]^2.$$

The IC and BCs as well as source term $f(x,y,t)$ are achieved from an exact solution $v(x,y,t) = \exp(x+y)t^2$.

The proposed method is adopted for solving this problem when the total time $T = 1$ with various values of h_x, h_y, τ and γ. Table 6 reports the maximum absolute errors L_∞ and time convergence orders C_τ for $h_x = h_y = \frac{1}{8}$, $\gamma \in \{0.65, 0.95\}$ and various values of τ. As shown in Table 6, the computational orders C_τ agree with the theoretical convergence order. Table 7 compares the maximum absolute errors L_∞ in the solution for $\gamma \in \{0.35, 0.75\}$ and several values of $h_x = h_y$ and τ. Table 8 lists the maximum absolute errors L_∞ in the solution for $\gamma = 0.2$ and several values of $h_x = h_y$ and τ. Table 9 makes the comparison of the maximum absolute errors L_∞ in the solution and execution times (in seconds) with those obtained with other schemes [22,25] for $h_x = h_y = \frac{1}{4}$ and $\tau = \frac{1}{256}$ and various values of γ. Figure 2 depicts the approximate solution and the associated computational error L_∞ of proposed method with $\gamma = 0.95$, $K_1 = K_2 = 16$, and $N = 256$.

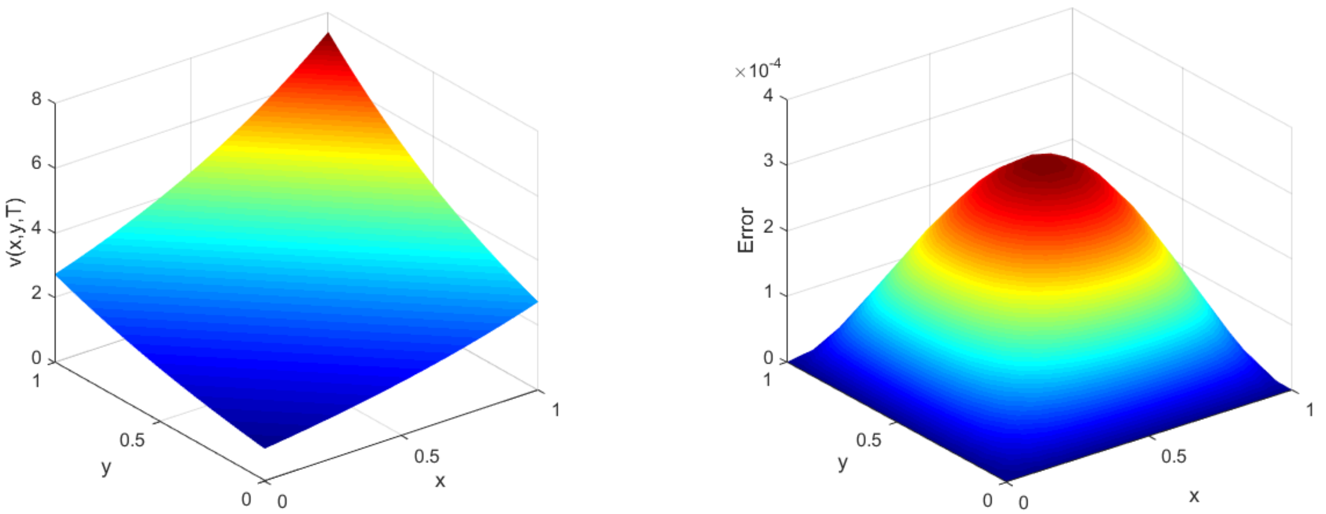

Figure 2. Approximate solution $v(x,y,T)$ and the associated computational error L_∞ of the proposed method with $\gamma = 0.95$ and $K_1 = K_2 = 16$ and $N = 256, n = 263$ (left and right panels, respectively).

Table 6. The maximum absolute errors L_∞ and time convergence orders C_τ of Example 2 for $h_x = h_y = \frac{1}{8}$, $\gamma \in \{0.65, 0.95\}$ and different values of τ.

τ	$\gamma = 0.55$			$\gamma = 0.85$		
	n	L_∞	C_τ	n	L_∞	C_τ
1/10	54	6.7051×10^{-3}	-	117	9.9156×10^{-3}	–
1/40	57	1.5503×10^{-3}	1.0563	34	8.5430×10^{-3}	0.1075
1/90	52	6.9213×10^{-4}	0.9944	31	1.0942×10^{-3}	2.5342
1/190	45	3.3634×10^{-4}	0.9658	22	5.1960×10^{-4}	0.9967
1/1200	21	7.7520×10^{-5}	0.7963	25	8.3012×10^{-5}	0.9951

Table 7. The maximum absolute errors L_∞ of Example 2 for $\gamma \in \{0.35, 0.75\}$ and different values of $h_x = h_y$ and τ.

h_x	τ	$\gamma = 0.35$		$\gamma = 0.75$	
		n	L_∞	n	L_∞
1/4	1/8	160	9.9757×10^{-3}	8	8.0374×10^{-3}
1/8	1/8	151	3.8090×10^{-3}	73	7.0374×10^{-3}
1/16	1/8	486	4.4059×10^{-3}	290	3.0374×10^{-3}
1/8	1/64	88	3.1647×10^{-4}	46	1.1573×10^{-3}
1/12	1/64	283	3.1281×10^{-4}	116	1.1583×10^{-3}
1/4	1/12	11	7.5942×10^{-4}	7	4.8539×10^{-4}
1/15	1/128	947	1.6066×10^{-5}	160	1.8297×10^{-4}
1/8	1/30	95	6.4711×10^{-4}	51	2.4751×10^{-3}
1/60	1/16	740	1.9589×10^{-3}	243	2.8112×10^{-3}

Table 8. The maximum absolute errors L_∞ of Example 2 for $\gamma = 0.2$, and several values of $h_x = h_y$ and τ.

h_x	τ	Proposed Method		Implicit Method [25]
		n	L_∞	L_∞
1/4	1/50	9	7.0500×10^{-4}	2.0154×10^{-3}
1/8	1/128	84	8.8460×10^{-5}	1.3776×10^{-4}
1/16	1/32	55	2.0142×10^{-3}	2.1391×10^{-3}

Table 9. The maximum absolute errors L_∞ and execution times (in seconds) of Example 2 for $h_x = h_y = \frac{1}{4}$ and $\tau = \frac{1}{256}$ and different values of γ.

γ	Proposed Method			Implicit Method [25]	
	n	L_∞	CPU Time (s)	L_∞	CPU Time (s)
0.18	8	9.2879×10^{-4}	1.4274	3.2350×10^{-3}	0.5373
0.35	6	4.9674×10^{-4}	1.5169	3.2306×10^{-3}	0.5397
0.70	3	7.8135×10^{-4}	1.5070	3.2302×10^{-3}	0.5719
0.80	4	2.3660×10^{-3}	1.4007	3.2368×10^{-3}	0.5651
0.90	3	3.0465×10^{-3}	1.3906	3.2457×10^{-3}	0.5102

6. Concluding Remarks

We adopted the predictor–corrector method for approximating the TFRSE. First, the time discretization of the problem was accomplished by using the finite difference. Second, the space discretization was obtained with the help of the predictor–corrector method. The convergence and unconditional stability properties of the approach were discussed theoretically. Numerical experiments compared the results obtained with the proposed method and those produced using existing alternative schemes. The superiority of the new approach was thus verified and illustrated.

Author Contributions: Conceptualization, L.D.L. and O.N.; data curation, B.M. and L.D.L.; formal analysis, B.M., O.N. and Z.A.; investigation, L.D.L. and O.N.; methodology, B.M., L.D.L. and A.M.L.; software, B.M. and O.N.; supervision, Z.A. and A.M.L.; validation, B.M., O.N. and Z.A.; visualization, B.M. and O.N.; writing—original draft, B.M. and O.N.; writing—review and editing, Z.A. and A.M.L. All authors have read and agreed to the published version of the manuscript.

Funding: The author Le Dinh Long is supported by Van Lang University.

Institutional Review Board Statement: Not applicable.

Informed Consent Statement: Not applicable.

Data Availability Statement: Not applicable.

Conflicts of Interest: The authors declare no conflict of interest.

References

1. Milici, C.; Drăgănescu, G.; Machado, J.T. *Introduction to Fractional Differential Equations*; Springer: Berlin/Heidelberg, Germany, 2019; Volume 25.
2. Biswas, K.; Bohannan, G.; Caponetto, R.; Lopes, A.M.; Machado, J.A.T. *Fractional-Order Devices*; Springer: Berlin/Heidelberg, Germany, 2017.
3. Qi, F.; Qu, J.; Chai, Y.; Chen, L.; Lopes, A.M. Synchronization of incommensurate fractional-order chaotic systems based on linear feedback control. *Fractal Fract.* **2022**, *6*, 221. [CrossRef]
4. Chen, L.; Li, X.; Chen, Y.; Wu, R.; Lopes, A.M.; Ge, S. Leader-follower non-fragile consensus of delayed fractional-order nonlinear multi-agent systems. *Appl. Math. Comput.* **2022**, *414*, 126688. [CrossRef]
5. Sabatier, J.; Agrawal, O.P.; Machado, J.T. *Advances in Fractional Calculus*; Springer: Berlin/Heidelberg, Germany, 2007; Volume 4.
6. Gutiérrez, R.E.; Rosário, J.M.; Tenreiro Machado, J. Fractional order calculus: Basic concepts and engineering applications. *Math. Probl. Eng.* **2010**, *2010*, 375858. [CrossRef]
7. Nikan, O.; Avazzadeh, Z. Numerical simulation of fractional evolution model arising in viscoelastic mechanics. *Appl. Numer. Math.* **2021**, *169*, 303–320. [CrossRef]
8. Qiu, W.; Xu, D.; Guo, J.; Zhou, J. A time two-grid algorithm based on finite difference method for the two-dimensional nonlinear time-fractional mobile/immobile transport model. *Numer. Algorithms* **2020**, *85*, 39–58. [CrossRef]
9. Xu, D.; Qiu, W.; Guo, J. A compact finite difference scheme for the fourth-order time-fractional integro-differential equation with a weakly singular kernel. *Numer. Meth. Part Differ. Equ.* **2020**, *36*, 439–458. [CrossRef]
10. Farnam, B.; Esmaeelzade Aghdam, Y.; Nikan, O. Numerical investigation of the two-dimensional space-time fractional diffusion equation in porous media. *Math. Sci.* **2021**, *15*, 153–160. [CrossRef]
11. Qiu, W.; Xu, D.; Guo, J. The Crank-Nicolson-type Sinc-Galerkin method for the fourth-order partial integro-differential equation with a weakly singular kernel. *Appl. Numer. Math.* **2021**, *159*, 239–258. [CrossRef]
12. Aghdam, Y.E.; Mesgrani, H.; Javidi, M.; Nikan, O. A computational approach for the space-time fractional advection–diffusion equation arising in contaminant transport through porous media. *Eng. Comput.* **2021**, *37*, 3615–3627. [CrossRef]
13. Qiu, W.; Xu, D.; Guo, J. Numerical solution of the fourth-order partial integro-differential equation with multi-term kernels by the Sinc-collocation method based on the double exponential transformation. *Appl. Math. Comput.* **2021**, *392*, 125693. [CrossRef]
14. Nikan, O.; Avazzadeh, Z.; Machado, J.T. Numerical approach for modeling fractional heat conduction in porous medium with the generalized Cattaneo model. *Appl. Math. Model.* **2021**, *100*, 107–124. [CrossRef]
15. Wenchang, T.; Wenxiao, P.; Mingyu, X. A note on unsteady flows of a viscoelastic fluid with the fractional Maxwell model between two parallel plates. *Int. J. Non-Linear Mech.* **2003**, *38*, 645–650. [CrossRef]
16. Hayat, T.; Nadeem, S.; Asghar, S. Periodic unidirectional flows of a viscoelastic fluid with the fractional Maxwell model. *Appl. Math. Comput.* **2004**, *151*, 153–161. [CrossRef]
17. Heymans, N. Fractional calculus description of non-linear viscoelastic behaviour of polymers. *Nonlinear Dyn.* **2004**, *38*, 221–231. [CrossRef]
18. Shen, F.; Tan, W.; Zhao, Y.; Masuoka, T. The Rayleigh–Stokes problem for a heated generalized second grade fluid with fractional derivative model. *Nonlinear Anal. Real World Appl.* **2006**, *7*, 1072–1080. [CrossRef]
19. Mainardi, F. *Fractional Calculus and Waves in Linear Viscoelasticity: An Introduction to Mathematical Models*; World Scientific: Singapore, 2010.
20. Qi, H.; Xu, M. Unsteady flow of viscoelastic fluid with fractional Maxwell model in a channel. *Mech. Res. Commun.* **2007**, *34*, 210–212. [CrossRef]
21. Xue, C.; Nie, J. Exact solutions of the Rayleigh–Stokes problem for a heated generalized second grade fluid in a porous half-space. *Appl. Math. Model.* **2009**, *33*, 524–531. [CrossRef]
22. Chen, C.M.; Liu, F.; Anh, V. Numerical analysis of the Rayleigh–Stokes problem for a heated generalized second grade fluid with fractional derivatives. *Appl. Math. Comput.* **2008**, *204*, 340–351. [CrossRef]
23. Wu, C. Numerical solution for Stokes' first problem for a heated generalized second grade fluid with fractional derivative. *Appl. Numer. Math.* **2009**, *59*, 2571–2583. [CrossRef]
24. Lin, Y.; Jiang, W. Numerical method for Stokes' first problem for a heated generalized second grade fluid with fractional derivative. *Numer. Methods Partial. Differ. Equations* **2011**, *27*, 1599–1609. [CrossRef]
25. Mohebbi, A.; Abbaszadeh, M.; Dehghan, M. Compact finite difference scheme and RBF meshless approach for solving 2D Rayleigh–Stokes problem for a heated generalized second grade fluid with fractional derivatives. *Comput. Methods Appl. Mech. Eng.* **2013**, *264*, 163–177. [CrossRef]
26. Zaky, M.A. An improved tau method for the multi-dimensional fractional Rayleigh–Stokes problem for a heated generalized second grade fluid. *Comput. Math. Appl.* **2018**, *75*, 2243–2258. [CrossRef]
27. Shivanian, E.; Jafarabadi, A. Rayleigh–Stokes problem for a heated generalized second grade fluid with fractional derivatives: A stable scheme based on spectral meshless radial point interpolation. *Eng. Comput.* **2018**, *34*, 77–90. [CrossRef]
28. Hafez, R.M.; Zaky, M.A.; Abdelkawy, M.A. Jacobi Spectral Galerkin method for Distributed-Order Fractional Rayleigh-Stokes problem for a Generalized Second Grade Fluid. *Front. Phys* **2020**, *7*, 240. [CrossRef]
29. Safari, F.; Sun, H. Improved singular boundary method and dual reciprocity method for fractional derivative Rayleigh–Stokes problem. *Eng. Comput.* **2020**, *37*, 3151–3166. [CrossRef]

30. Nikan, O.; Golbabai, A.; Machado, J.T.; Nikazad, T. Numerical solution of the fractional Rayleigh–Stokes model arising in a heated generalized second-grade fluid. *Eng. Comput.* **2021**, *37*, 1751–1764. [CrossRef]
31. Khan, M.A.; Ali, N.H.M. High-order compact scheme for the two-dimensional fractional Rayleigh–Stokes problem for a heated generalized second-grade fluid. *Adv. Differ. Equ.* **2020**, *2020*, 233. [CrossRef]
32. Naz, A.; Ali, U.; Elfasakhany, A.; Ismail, K.A.; Al-Sehemi, A.G.; Al-Ghamdi, A.A. An Implicit Numerical Approach for 2D Rayleigh Stokes Problem for a Heated Generalized Second Grade Fluid with Fractional Derivative. *Fractal Fract.* **2021**, *5*, 283. [CrossRef]
33. Yuste, S.B. Weighted average finite difference methods for fractional diffusion equations. *J. Comput. Phys.* **2006**, *216*, 264–274. [CrossRef]